Study of Physical Interactions of Silver Nanoparticles with Human Insulin for its Diabetes Related Wound Healing Activity

Thesis is submitted in partial fulfilment of the requirements
For the award of the degree of
Masters in science
In
Chemistry

Submitted By:
Pawandeep Kaur
Roll No. 301402015

Under the guidance of
Dr. Diptiman Choudhury
to the

School of Chemistry and Biochemistry
Thapar University
Patiala-147004 (Punjab)
INDIA
July 2016

Candidate's Declaration

I hereby declare that the work being presented in the dissertation entitled "Study of Physical Interactions of Silver Nanoparticles with Human Insulin for its Diabetes Related Wound Healing Activity" in the partial fulfilment of the requirements for the award of the degree of Masters in Chemistry, School of Chemistry and Biochemistry, Thapar University, Patiala, is my own work during the period of January to July 2016, under the supervision of Dr. Diptiman Choudhury. My thesis has not previously formed the basis for award of any degree, or other, or other similar title or recognition.

Pawandeep Kaur

Pawandeep Kaur

Patiala
Date: 15-july-2016

This is to certify that the above statement made by the candidate is correct and true to the best of my knowledge.

Dr. Diptiman Choudhury
Project Supervisor
Assistant Professor (SCBC)
TU, Patiala

Dr. Bonamali Pal
Head of SCBC
TU, Patiala

Certificate

This is certify that the project entitled "Study of Physical Interactions of Silver Nanoparticles with Human Insulin for its Diabetes Related Wound Healing Activity" being submitted by Ms. Pawandeep Kaur in partial fulfilment of requirement for the award of the degree of Masters of Science in School of Chemistry and Biochemistry, Thapar University, Patiala, is a bonified work carried out under the supervision of Dr. Diptiman Choudhury and no part of this project has been submitted for award of any degree by me.

Dr. Diptiman Choudhury
Assistant Professor (SCBC)
TU, Patiala

Dr. Bonamali Pal
Professor and Head (SCBC)
TU, Patiala

Dr. S.S. Bhatia
Dean of Academic Affairs
TU, Patiala

Acknowledgement

To make a project successful, there are many helping hands. I would like to express my sincere gratitude and appreciation to many people who helped keep me on track toward the completion of my project.

Firstly, I express my sincere thanks to **Dr. Diptiman Choudhury,** for providing exemplary guidance all necessary facilities, full co-operation, monitoring and constant encouragement throughout the course of this project work. The blessing, help and guidance given by him time to time shall carry me a long way in the journey of life on which I am about to embark.

I want to express my gratitude to **Dr. Gopal Chakrabarti,** head of department of biotechnology of Calcutta university, for providing me with best facilities in the department, full co-operation, continued encouragement and his timely valuable suggestions. I am thankful to Mr. Arnab ganguli, Dr. Amlan Das and Mr. Devasish Nag for their valuable contribution in this project work.

I am obliged to **Dr. Soumen Basu** for his cordial support, his valuable suggestions, motivation and guidance during project work. I am grateful to all laboratory staff for their cooperation during the period of my assignment, which helped me in completing this task through various stages. In my daily work I have been blessed with a friendly and cheerful group of research scholar Ms. Vanshita Goel.

I owe the biggest thanks and sense of gratitude to **Dr. Bonamali Pal** and **other faculties of SCBC** for guiding me and providing me support whenever I needed.

I wish to express my gratitude to my parents and friends for their encouragement and blessings which supported me throughout this, without which this project would not possible.

Pawandeep kaur

Pawandeep Kaur

List of Contents

Abstract

Green synthesis of AgNPs was done at pH 7.4 by aqueous extract of tulsi leaves (TAE) under sunlight. Thereafter insulin coating of the AgNPs were done by incubating with recombinant human insulin at physiological conditions (temperature 37°C and pH 7.4) for an hour. The physical interactions of AgNPs with insulin was studied by using UV-visible spectroscopy, Dynamic Light Scattering (DLS), Zeta potential measurement, Tyrosine intrinsic fluorescence, far UV Circular Dichroism (far UV-CD), Fourier Transform Infrared spectroscopy (FTIR), Raman spectroscopy, Field Emission Scanning Electron Microscope (FE-SEM) and Transmission electron microscope (TEM). The Thermodynamic kinetics was studied from time and concentration dependent fluorescence spectra shows the reaction was most favourable at 37°C with ΔG -7.48 kcal/mole and ΔS 0.76 kcal/mole K^{-1} indicates that the reaction is endothermic with activation energy 3.84 Kcal $mole^{-1}$and rate constant 604,500 s^{-1}. The wound healing activity was checked out by cell migration of lung epithelial cell line in presence of 3.0 pM and 60 pM insulin protected AgNPs (IAgNPs), in media containing different glucose concentration (100, 180 and 360 mg/dl), shows the effective migration takes place in the presence of nanoparticles and after 24 hours the cell culture containing 60 pM IAgNPs healed up completely.

Review of literatures

Wound is loss of continuity of epithelium, with or without the loss of underlying connective tissue (i.e. muscle, nerves, and bones) due to an injury.[1] Injury can either be internal or external. External injury can cause by mechanical (friction or shear force, pressure, electrical, heat or cold), chemical, or radiation source. Injury stimulates a series of events to restore tissue integrity. Depending on the severity and size of the wound several physiological and metabolic changes occurs resulting impaired wound healing and increased morbidity of tissue.[2]

Wounds classified into open or closed type and diabetic wounds. Closed wounds are the result of friction of surfaces with each other, these wound does not break through the skin and may includes abrasions, laceration, contusion (swallow bruises due to accumulation of blood and dead cells under skin) and concussions (underlying organs and tissue on head with no significant external wound), But open type wounds caused by sharp edge object, blunt trauma, abrasions, avulsions, puncture wounds, if reaching down to the underlying tissue and organs, includes stab wound, skin cuts, surgical wounds and gunshot wounds or miscellaneous wounds, also involves thermal wounds (like burns, sunburns and frostbite), chemical wounds (causes skin or lung damage) and electrical wounds. Open wounds exposes the underlying tissue to outside environment and are prone to infections resulting in activations of inflammatory responses causing formation of gangrenes which may be disabling and life threatening if major organ such as blood vessel, nerve system damaged and hepatic system get involved.[3, 4] Diabetes is a metabolic disorder characterized by chronic hyperglycemia with disturbances of carbohydrate, fat and protein metabolism and glucose homeostasis.[5]

In normal wound healing, a complex dynamic process involves molecular and physiological processes. To repair and regenerate the tissue cellular and biochemical events like haemostasis, inflammation, proliferation, epithelisation, maturation and remodelling of scar tissue occurs.[6,7,8] Haemostasis or clot formation involves exposure of sub endothelial collagen to platelets located to intravascular space, collagen forms thrombin which activates the platelets changes to amorphous shape, form fibrin clot to prevent bleeding.[9,10] Then platelet degranulation takes place, platelet α-granules releases growth factors which causes inflammation[11,12] and proliferation phase is characterised by the formation of primary cells, fibroblast and endothelial cells, these proliferate in response to growth factors, fibroblast releases collagen and fibronectin to form ECM (extracellular matrix) for re-epithelialisation of epidermis and angiogenesis occur.[13] Re-epithelisation requires junction between the epidermis and dermis.[14] The growth factors include IGF (insulin like growth factor includes IGF-1 and IGF-2), EGF (epidermal growth factor), TGA-α (transforming growth factor alpha), Hb-EGF (heparin binding epidermal growth factor), Amphirgulin, TGF-β (transforming growth factor beta), PDGF (platelet derived growth factor), VEGF (vascular endothelial growth factor) and KGF (keratinocyte growth factor).[11,12]In case of diabetic wounds, delayed healing. Healing problems are caused by the peripheral arterial disease and peripheral neuropathy that occur with diabetes, wherein the

blood vessels in different parts of the body (hands and feet), grow narrower and reduce the blood circulation to those areas. A lack of circulation in the extremities can result in reduced supply of oxygen and nutrients the body tissue and blood also contain high glucose, wounds often go unnoticed by diabetic patient, delayed treatment can put the patient at the risk for further complications and it also leads to decrease in secretion of growth factors.[15] In case of lung cancer patients, diabetes mellitus beneficial, the patients survived more than without diabetes mellitus. [16] Lung cancers, called carcinoma or metastasis breast cancer, spread to brain, bone, liver, kidney and opposite lung.[17] To treat lung cancer Insulin like Growth Factor Inhibitor (IGF inhibitor) therapy used, in diabetic patients Insulin Like Growth Factor production decreases due to this cell formation decreases.[16]

IGF is an important growth factor produced by fibroblast cells, macrophages and platelets, promotes the migration of endothelial cells into the wound and induce the proliferation or mitosis of fibroblast cells for the formation of ECM and angiogenesis by activating the protein kinase B signalling pathway, also catalyze skeletal muscle hypertrophy by inducing protein synthesis and by blocking muscle atrophy.[18,19] IGF protein shows 48% sequence similarity to proinsulin, has positions 1 to 29 similar to B chains and positions 42 to 62 are similar to insulin A chain but "connecting peptide" positions 30 to 41 shows no homology to proinsulin C peptide, cross linked by three disulphide bridges.[20] Insulin, a peptide hormone produced by beta cells of islets of langerhans of pancreas primarily known for anti-glycemic activity, regulates the metabolism of carbohydrates and fat by promoting the absorption of glucose from blood to skeletal muscles , control the blood sugar level and used to treat diabetes milletes.[21] The structural similarity shows that insulin performs biological functions, re-epithelialisation like IGF.[22,23] The insulin also causes the proliferation of fibroblast cells, that are critically involved in the angiogenesis and formation of ECM, suggested that insulin acts as the growth homone.[24]

Through open wounds the invading microbes like *Escherichia Coli, Staphylococcus aureus, Bacillus subtilis, Salmonella typhi, Acinetobacter bauminnii, S. Epidermis, S. Pyogenes* and *P. Aeruginosa* etc, causes infection, stimulate to diapedesis and also the Growth factors present in tissue surrounding the wound to draw chemotactically inflammatory cells like neutrophils and monocytes etc into the injured area.[11, 12] Neutrophils, Monocytes, Eosinophils etc are phagocytes. Neutrophils release hydrolytic lysosomal enzymes such as elastase, neutral protease and collagenase for the lysis of microbes and causes inflammation, redness, bleeding and loss or impairment of function of wounded area.[13, 14,]Chemical antiseptics include Hydrogen Peroxide, Quaternary Ammonium compounds, Alcohols, Sodium Bicarbonate etc are used to kill microbes, different types of bacteria differ in susceptibility towards antiseptics[25], the low concentration of antiseptics encourage growth of resistant bacteria but at high concentration causes tissue damage and slow wound healing. Alternative to this, silver based antimicrobials includes Silvercell™ - J&J , Aquacell™ – convatec and nanocystalline silver (Acticoat™ – Smith & Nephew).[26] Within the cells the silver starts accumulate introduce into bacterial cell wall, lysis it by inducing high degree of structural (pores and pits),

morphological changes and interact with phosphate-containing compounds (like DNA and RNA) inhibit their replication, sulphur containing proteins on the membrane and poisons the respiratory enzymes.[27, 28]

Silver nanoparticles are of size between 1nm and 100nm and numerous shapes like spherical, rods, diamond, octahedral and thin sheets.[29] The most common applications of silver nanoparticles includes catalysis[30], photocatalysis[31], for oxidation (benzene to phenol[31] and carbon monoxide[32]), in chemotherapy[32] and as carrier for delivering the drug molecules or large molecules to specific targets and as antimicrobial agents.[33] various parts of the plants are rich in naturally occurring Polyphenolic compounds such as neem, datura, grapes, *Aloe vera*, ginger and garlic etc.[34, 35]

Tulsi plant (*Ocimum tenuiflorum*) among them which is full of naturally occurring polyphenols, well known for its antimicrobial activity.[36] Tulsi has main components oleanolic acid, ursolic acid, Rosmarinic acid, Eugenol, Carvacrol, Linalool, β-Caryophyllene, β-Elemene and Germacrene D.[37,38] Oleanolic acid has antimicrobial or antiviral activity, Rosmarinic acid acts as anti-bacterial agent and eugenol has germicidal activity.[39] It has antibacterial activity against *Enterobacter cloacae, Escheria Coli*, *Staphylococcus aureus, Proteus vulgaris, Proteus mirabilus* and *Pseudomonas aeruginosa.*.[36, 39]

In this project, green synthesis of silver nanoparticles (AgNPs) was carried out by using green tulsi leaf extract (pH 7.4) as reducing and capping agents in the presence of sunlight. Then AgNPs were protected with insulin by incubating at physiological pH and temperature.

Objectives

To the best of knowledge so far many green methods to synthesize AgNPs, also using tulsi leaf extract synthesis of AgNPs has been already known in literature but the synthesis of IAgNPs not yet known. As part of our continuing research program aimed:

1. At developing an efficient synthetic approach for the synthesis of IAgNPs.
2. Study the Physical interaction of AgNPs with Human recombinant Insulin.
3. Check the Diabetic wound healing activity of IAgNPs.

Material and Methods

Materials

Bovine Serum Albumin (BSA), Formaldehyde, Glucose, DMEM-F12, 100 X Penicillin-streptomycin mixture, Sodium bicarbonate, Silver nitrate, Lead acetate, Hydrochloric acid and Sodium hydroxide were purchased from Himedia, India. Human recombinant insulin (Huminsulin) was purchased from Eli Lilly and com, India, *Ocimum tenuiflorum* (Tulsi leaves) leafs were cultivated and harvested from university research field. All chemicals used were of molecular biology grade.

Preparation of tulsi extract

Ocimum tenuiflorum (tulsi) leaf extract was prepared by boiling 3 g of tulsi leaves in 100 ml water for 2 hours. After cooling, pH of the solution was adjusted to 7.4 by using 0.01 N NaOH and extract was filtered using Watsman No.1 filter paper to remove particulate matter and to get clear solution (TAE) and preserved at 4°C further experiments.

Preparation of Silver nanoparticles and insulin protected AgNPs

Green synthesis of AgNPs was carried out by using TAE pH 7.4 as a capping and reducing agent. $AgNO_3$ (240 µM) 125 µl was added in 4875 µl of TAE. Thereafter the mixture was kept under sunlight for 10 minutes. The colour of solution changed from faint light yellow to reddish brown in the presence of sunlight, indicated the formation of AgNPs. The change of colour was due to excitation of surface vibrations by silver nanoparticles. After this, AgNPs were incubated with insulin 60 pM (1:50 AgNPs: insulin) at physiological conditions, pH (7.4) and temperature (37°C) in an incubator for an hour.

Characterization

Absorbance spectra

After synthesis of TAE protected AgNPs and insulin IAgNPs UV-visible spectral absorbance was measured using Analytic Jena UV-Visible spectrophotometer, operated between 600 to 280 nm wavelength ranges. Interaction between AgNPs and BSA protein also checked out.

Dynamic Light Scattering and Zeta potential

DLS used for characterizing the size of colloidal dispersion, utilizes the illumination of a suspension of particles undergoing Brownian motion by laser beam. Brookhaven 90 plus (particle size analysis) used to determine average hydrodynamic size of bio reduced AgNPs, IAgNPs and also of AgNPs with BSA hydrodynamic size determined. Stability and charge of IAgNPs was monitored spectroscopically by using Malvern v2.3 Zeta potential analyzer.

Far UV circular dichroism (Far UV-CD)

Far UV CD absorption is used to determine the secondary conformational changes of insulin protein after incubation with AgNPs or effect of AgNPs on secondary structure of

insulin. The far-UV CD measurements were carried out between at wavelength range from 260 to 200 nm with Jasco (model J-815) CD spectrometer, using 0.1 cm path length quartz cuvette. CD spectra were taken at 37°C for 20 minutes by incubating AgNPs (0.0248 x 10^{-3} µM)) with insulin (14.99 µM) to observe the secondary structure conformational changes of the protein.

FTIR spectrometer

The binding of AgNPs with TAE was done by using Cary 600 series FTIR spectrometer. The sample solution containing AgNPs were washed to remove all other bioinorganic matter present in solution. Clean green AgNPs sample was incubated with insulin. At 37 °C the samples of control (TAE and insulin), AgNPs and IAgNPs were air dried. The sample pellets prepared by mixing samples with potassium bromide (KBr). FTIR analysis (4000-500 cm^{-1}) carried out to check the functional groups involved in interactions.

Raman spectrometer

Surface Enhanced Raman Scattering (SERS) spectra were observed with Raman spectrometer having laser 532 nm. Samples were prepared as before. Samples were dried by spreading (50 µl) over the glass cover slips and incubated at 37°C for 1 hour. Raman analysis (1900-200 cm^{-1}) was done to check the functional groups involved in interactions.

Fluorescence spectrometer

Photon Technology International Fluorescence spectrophotometer with a variable temperature Peltier system was used for fluorescence measurements, to determine the binding stoichiometry, dissociation constant and association constant of insulin with AgNPs at different temperatures i.e. 37°C, 32°C, and 27°C using 400 µl quartz cuvette of 1 cm path length. Operated with excitation at 280 nm for tyrosine residue of insulin and emission scan range 285 to 350 nm, with excitation and emission slit of 5 mm. The inner filter effect was corrected by using equation (1).

$$Fcorr = Fmax \text{ antilog } [(Aex+Aem)/2] \qquad (1)$$

Aex is the absorbance of excitation wavelength and Aem is the absorbance at emission wavelength.[37]The absorbance measurements were performed with JASCO V-630 UV-Visible spectrophotometer using 1 cm path length quartz cuvette. The binding stoichiometry of insulin was determined using scatchared plot, keeping the constant concentration of insulin (5 µM) but varying the AgNPs concentration from 2 µl (0.062 x 10^{-3} µM to 0.031 x 10^{-3} µM) till 15 minutes at three different temperatures 27°C, 32°C and 37°C. The fraction of binding sites (R) occupied was determined by using equation (2).

$$R = [F_o - (F)] / Fmax \qquad (2)$$

Where F_o is the corrected fluorescence intensity in the absence and F is the corrected fluorescence in the presence of ligand. The Fmax was calculated from the plot of $1/[F_o - (F)]$ versus 1/ concentration of ligand (AgNPs), then used to determine binding sites. Then

R versus R/Lf plot was used to determine the association constant (K_a), dissociation constant (K_d) and stoichiometry of protein to ligand binding. Where Lf represents the free ligand concentration and Lf was determined using equation (3).

$$Lf = Co - Lb \qquad (3)$$

Where Co is ligand initial concentration and Lb is the concentrations of ligand after binding with insulin respectively. Lb calculated using equation (4).

$$Lb = R * \text{concentration of protein} \qquad (4)$$

Calculated values of K_a values at different temperatures, used for van't Hoff plot for the analysis of thermodynamic parameters of binding of insulin with AgNPs, ΔG, ΔH, TΔS and ΔS. The slope of plot ln (K_a) versus 1/Temperature (at 27°C, 32°C and 37°C) gives ΔH value using Van't Hoff equation (5).

$$\ln (Ka) = + (\Delta S/R) - (\Delta H/RT) \qquad (5)$$

From this plot, -ΔH/R is the slop and ΔS/R is the intercept of linear fit, from the intercept the enthalpy of the reaction easily obtained and from equation (6) and (7), Gibbs free energy and entropy was calculated respectively.

$$\Delta G = - RT\ln (K_a) \qquad (6)$$
$$\Delta S = (\Delta H - \Delta G)/T \qquad (7)$$

R is the ideal gas constant.

The time dependent quenching of fluorescence was studied of insulin (5 μM) with AgNPs (0.031×10^{-3} μM) till 15 minutes to determine the order of the reaction and activation energy using Arrhenius equation (8) by plotting ln K_a versus 1/ temperature.

$$\ln K = - E_a/R (1/T) + \ln A \qquad (8)$$

Where E_a is activation energy, K is the rate constant and A is the Arrhenius constant.[40]

Field Emission Scanning Electron Microscope (FE SEM)

The surface morphology and size of the nanoparticles before and after interaction with insulin was monitored using Field Emission Scanning Electron Microscope (Joel, JSM, model 7600 F), accelerated at voltage 15 KV. 2mm platinum surface coating was done by using Quarum (model Q150 T) before scanning the samples.

Transmission Electron Microscope (TEM)

The morphology, particle size and size distribution of the biosynthesised AgNPs and IAgNPs were studied by using Transmission Electron Microscope Hitachi (H-7500).

AgNPs and IAgNPs solution were placed on carbon coated copper TEM grids (400 mesh), to stain the insulin protected AgNP's; (0.25%) lead acetate solution of pH 11.98 was used.

Cell migration assay

Human lung epithelial cell line (carcinoma), A549 was used to check the wound healing activity of IAgNPs in normal glycemic and hyper glycemic conditions. DMEM-F12 culture media was supplemented with 10% calf serum and 1X antibiotic (penicillin-streptomycin) and filter sterilized before use. Calculated amount of dextrose was supplemented to make hyper glycemic media (containing 180 and 360 mg/dl). A549 cell were maintained and treated in humidified cell culture incubator at 37°C and 5% CO_2. A549 cell were grown in monolayer condition at 90-95% confluence, before generating wound by scratch method. After creation of wound cells were supplemented with 3 pM and 60 pM of IAgNPs. Time depended wound healing activity was monitored till 24 h under microscope.

Results and discussion

Absorbance spectra

Tulsi capped AgNPs showed sharp absorbance peak with maximum at 352 nm wavelength indicated the reduction of $AgNO_3$ into Silver nanoparticles with spherical shape. IAgNPs also showed shape absorption peak with absorption maxima at 349 nm; suggesting mono dispersity of the particles. Blue shift (3 nm) may suggest better protection of AgNP particles in presence of insulin. In case of BSA, no interaction between AgNPs and BSA this is confirmed by DLS and CD data also. (Figure 1)

Dynamic Light Scattering and Zeta potential

DLS data showed the bioreduced AgNPs and IAgNPs have average hydrodynamic size approximately 22 ± nm and 42 ± nm respectively. The zeta potential value of IAgNPs has a sharp peak with –ve value, suggests that the IAgNPs has negative charge at the surface; negative charge confirms the repulsion among the nanoparticles and proves that they are very stable and dispersed in medium. With BSA the size approximately similar to AgNPs, showed no interaction. (Figure 2)

AgNPs : Insulin	Zeta potential (mV)	Result quality
AgNPs (only)	-12.4	Good
1:50	-13.4	Good
1:500	-15.1	Good
1:5000	-15.2	Good

Far UV circular Dichroism (Far UV-CD)

The absorbance of buffer and buffer with insulin was subtracted from insulin and AgNPs-insulin spectra. The insulin control has –ve band maxima, at 207 nm and absorbance minima at 210 nm with mean residue ellipticity -4.9, -3.6 and -3.1 deg cm^2 $decimole^{-1}$ respectively indicates that native insulin is helical, after 5 to 20 minutes the –ve strong band appear at 208 nm with mean residue ellipticity -6.8 deg cm^2 $decimole^{-1}$, suggesting AgNPs induce the helicity and more stabilize the secondary structure of insulin than native insulin but no changes in BSA structure. (Figure 3)

FTIR spectra

FTIR measurements of control, biosynthesised AgNPs and IAgNPs was carried out through the potassium bromide pellets, biosynthesised AgNPs shows the prominent transmission peak of Amide-A peak at 3428 cm^{-1} (–NH and –OH stretch) and Amide-B at 2844 cm^{-1} (Aliphatic C-H stretch) which is at 3399 cm^{-1} and 2853 cm^{-1} respectively in tulsi extract control this shift in transmission peak shows that these functional groups strongly bind with silver metal and acts as stabilising and reducing agent for nanoparticles synthesis.

Amide-I peak at 1607 cm^{-1} (C=O and C-N stretch), Amide-II at 1403 cm^{-1}, Amide-III at 1206 cm^{-1} and 1058 cm^{-1} and Amide-IV at 814 cm^{-1} (Aromatic and alkenes =C-H stretch) are not prominent in biosynthesised AgNPs suggesting that these functional groups are less contributing towards AgNPs synthesis.

In case of biosynthesised AgNPs and IAgNPs, functional groups having Amide-A, Amide-B, Amide-I, Amide-II, Amide-III, C=S peak at 1111 cm^{-1} and 1049 cm^{-1} and Amide-IV at 682 cm^{-1} and 550 cm^{-1} (C-S stretch) bonds prominent peaks in case of AgNPs protected with insulin in comparison with biosynthesised AgNPs indicates insulin strongly bind with AgNPs. In comparison with transmittance of control insulin, IAgNPs shows transmittance peak of Amide-A at 3397 cm^{-1}, Amide-B at 2886 cm^{-1}, Amide-I at 1653 cm^{-1}, Amide-II at 1458 cm^{-1} and 1417 cm^{-1} and most prominent peak of C=S functional group at 1111 cm^{-1} and 1049 cm^{-1} which differ from control insulin indicates that C=S functional group more strongly bound with AgNPs than other functional groups. (Figure 5)

Functional groups	**Tulsi extract (cm^{-1})**	**AgNPs (cm^{-1})**	**Insulin (cm^{-1})**	**IAgNPs (cm^{-1})**
Amide-A (-NH and –OH stretch)	3399	3428	-	3397
Amide-B (Aliphatic C-H stretch)	2853	2844	2939	2886
Amide-I (C=O and C-N stretch)	1629	1607	1658	1653
Amide-II	1403	1466	1412	1458, 1417
Amide-III (Ether linkage)	1119, 1058	1102, 1020	1228	1228
Amide-IV (Aromatic and Alkene =C-H stretch)	814	797,726	-	-

C-S (Stretch)	-	-	Broad band	550, 682
Nitrile (Stretch)	2356	2355	-	-

Raman spectra

Vibrational signals of Raman spectrum of Amide I peak at 1612 cm^{-1} of tulsi leaf extract shows shift towards lower wave number 1602 cm^{-1}, less energy required for excitation but in Amide II and Amide III peaks of tulsi extract capped AgNPs shows shift towards higher wave number value or higher energy shows that these are less exposed to surface or involved in binding with AgNPs.

The spectra of insulin shows that the major changes during after interaction with AgNPs, Amide III peaks at 1283 and 1316 cm^{-1} are absent in case of IAgNPs spectra and the peak present at 1249 cm^{-1} shows antistokes shift towards higher wave number 1265 cm^{-1} and also in case of insulin protected AgNPs peaks at 978 cm^{-1} antistokes shift from insulin, shows involved in binding with AgNP but peak at 918 cm^{-1} show shift towards lower wave number i.e. stokes shift, indicate that the vibrations takes place easily. The peak at 538 cm^{-1} in case of IAgNPs shift towards higher wave number, shows S-S linkage vibrations between the protein chains require more energy than in case of native protein indicate its involvement in binding with AgNP. (Figure 6)

Functional groups	**Tulsi extract (cm^{-1})**	**AgNPs (cm^{-1})**	**Insulin (cm^{-1})**	**IAgNPs (cm^{-1})**
Amide-I	1612	1602	1646,1636	1639
Amide-II	1400	1400	1449	1449
Amide-III (C-N and C=N stretch)	1261	1316	1283,1249	1265
Amide-IV	719	719	784	784
S-S bending	-	-	538	542

C-C bending	221	195	241	170
Other peaks (Unidentified peaks)		1597		
	1549	1548	-	1549
	307	311	310	307

Fluorescence spectra

The emission spectra are monitored at 320 nm with excitation at 280 nm. With different dose concentration of ligand, the changes in the intrinsic fluorescence of insulin after incubation with insulin at different temperatures determined, association constant (Ka) 72.8, 94.11 and 173.56 μM at 27°C, 32°C and 37°C respectively, dissociation constant (Kd) 13.7, 10.63 and 5.76 μM at 27°C, 32°C and 37°C respectively stoichiometric ratio of ligand to insulin is 1:1, 1:1 and 1:1.5 at 27°C, 32°C and 37°C respectively indicates that the association or interaction between protein and ligand is stable at 37°C. The plot of ln K_a versus 1/T, gives ΔH value is 16.08 kcal $mole^{-1}$ (ΔH>0) shows that the net enthalpy change is positive and ligand protein binding interaction is endothermic (heat is absorbed during reaction), ΔG is -6.72, -6.98 and -7.48 kcal $mole^{-1}$ at 27°C, 32°C and 37°C temperature respectively shows the ΔG more negative at 37°C indicates the reaction is forward, favourable and high affinity of binding of ligand with protein at 37°C and ΔS is 0.076 Kcal $mole^{-1}$ K^{-1} shows that reaction is entropically driven and positive value indicates that the solvation entropy is favourable but conformational degree of freedom is unfavourable. The time dependent insulin fluorescence quenching, indicates the reaction is of first order with rate constant 604500, 576000 and 492000 s^{-1} at 37°C, 32°C and 27°C respectively and the E_a is 3.84 Kcal $mole^{-1}$ shows the reaction is endothermic as shown by the ΔH value. The AgNPs reduced the intrinsic tyrosine fluorescence intensity of insulin by 5.39%, 12% and 12.6% with 0.0062, 0.0248 and 0.031 nM concentration of AgNPs respectively, after 10 minute incubation, shows with increase in concentration of ligand the loss of fluorescence intensity is more. (Figure 4)

Field Emission Scanning Electron Microscope (FE SEM)

FE SEM shows the size similarity with the DLS results, size distribution of AgNPs ranges from 8 to 40 nm with average 23 nm size and IAgNPs has average size around 38 to 45 nm with spherical shape. (Figure 7)

Transmission Electron Microscope (TEM)

TEM micrographs suggest that both AgNPs and IAgNPs are spherical in shape. AgNPs are of variable sizes, the size distribution ranges from 8 nm to 40 nm of AgNPs with average size 23 nm deduced from DLS data and capped with 3 to 4 nm wide tulsi extract coating, and the images of IAgNPs shows IAgNPs are more dispersed and stable than AgNPs as shown by zeta potential. (Figure 8)

Lung epithelial cell migration

Cell migration results showed that lung epithelial cells have migrated in response to insulin protected AgNPs. The amount of cell migration was more in the presence of IAgNPs than without nanoparticles. Extend of migration increased with increase of time and IAgNPs concentration. After 24 hours of incubation with (60 pM) IAgNPs showed complete healing up of monolayer wound, suggesting good efficiency of the particles. The phenomenon is true for both normal glycemic and hyper glycemic conditions. In media containing different glucose concentration (i.e. 100, 180 and 360 mg/dl) the cell migration took place effectively in comparison to control (untreated cells at respective glycemic conditions), suggesting effective wound healing activity of those nanoparticles in hyperglycaemic conditions which may suggest probable use of particles for treating diabetes related wounds. (Figure 9)

Conclusions

The results suggested that TAE protected AgNPs physically interacted with human recombinant insulin at normal physiological conditions. Different spectroscopic studies suggested that interaction of AgNPs leaded to some structural changes to the insulin protein. BSA was taken as control protein for studying the interactions. No significant structural alterations have been observed of the protein, suggesting specificity of the AgNP-insulin interactions. FTIR and Raman studies showed protein structural changes involved mostly alteration of Amide-I, II and III where as amide – IV, A and B remained unaltered. Probable use of the insulin capped AgNPs lies on its wound healing activity of in hyper glycemic conditions. It showed effective migration of lung epithelial cells in normal and hyper glycemic conditions. Persistent hyper-glycemic conditions in the body causes spontaneous wounds and also delays healing up process of pre-existing wounds. Moreover; Silver nanoparticles are known for its antibacterial activity. Therefore, successful exploitation of the insulin-AgNPs particles will be helpful to the diabetes patients to recover their tissue integrity in an infection free manner.

REFRENCES

1. D.J. Leaper and K.G. Harding. “Biology and Management”. *Oxford Medical Publications* - 1998.
2. D.P. Orgill, C. Blanco. “The Patho physiologic Basis for Wound Healing and Cutaneous Regeneration”. *Science* - 2009: 25-57.
3. T. Velnar, T. Bailey, V. Smrkolj. “The Wound Healing Process: An Overview of the Cellular and Molecular Mechanism”. *National Center for Biotechnology Information PubMed* - 2009; **37**: 1528-1542.
4. B. Paulline. “Basic Science of Wound Healing”. *Surgery (Oxford) on Science Direct* - 2010; **28**: T 409-412.
5. K. Maruyama, et al. “Decreased macrophage number and activation lead to reduced lymphatic vessel formation and contribute to impaired diabetic wound healing”. *American Journal Pathol*- 2007; **170:** 1178-1191.
6. Hunt, K. Thomas. “Basic principles of Wound Healing”. *Trauma and Acute Care Surgery* – 1990; **30**: 122-128.
7. W. Stadelmann, A. Digenis, G. Tobin. “Physiology and Healing Dynamics of Chronic Cutaneous Wounds”. *American Journal of Society* - 1998; **176**: 26S-38S.
8. Colman RW, Hirsh J, Marder VJ, et al. Hemostasis and Thrombosis. Basic Principles and Clinical Practice. *Philadelphia: Lippincott* - 1994.
9. M. Kurkinen, A. Vaheri, P. Robert. “Sequential appearance of Fibronectin and Collagen in Experimental Granulation Tissue”. *Lab Invest* - 1980; 43: 47-51.
10. J. Folkman, M. Klagsburn. “Angiogenic Factor”. *Science* - 1987; **235**: 442-447.
11. D. Simpson, R. Ross. “The Neucleophilic Leukocyte in Wound Repair: A study with antineutrophil serum”. *American Society for Clinical Investigation* - 1972; **51:** 2009-2023.
12. D. Cooper. “Optimising Wound Healing”. *Nurse Clinics of North America* - 1990; **25**: 165-180.
13. A. F. Haas. “wound healing”. *Dermatology Nurses’ Association* - 1995; **74**: 28-34.
14. K.S. Midwood, L A..V. Williams, J.E. Schwarzbauer. “Tissue Repair and Dynamic of Extracellular Matrix”. *International Journal of Biochemistry and Cell Biology* - 2004; **36**: 1031-1037.
15. M. Witte, A. Barbul. “General Principels of Wound Healing”. *Surgical clinics of North America* - 1997; 77: 509-528.
16. H. Peter, H.G. Bjorn, L. Arnulf, M.C. Carslen, A. Tore. “Prolonged Survival in Patients with Lung Cancer with Diabetes Mellitus”. *Journal of Thoracic Oncology* – 2011; **6**: 1810-1817.
17. B.S. Joon, G.I. Jung, J.C. Myung, K.Y. Mi. “Atypical Pulmonary Metatases: Spectrum of Radiologic Findings”. *Radiographics* – 2001; **21**: 403-417.
18. E.B. Karin, J.A. Hans, H.D. Hans, S. Anna, E.S. Jarl. “Receptor for Insulin Like Growth Factor I in Plasma Membrane Isolated from Bovine Mesenteric Arteries”. *Acta Endocrinol* - 1998; **117**: 428-434.
19. A.C. Moses, S.C. Young, L.A. Morrow, M. O’Brien, D.R. Clemmons. “Recombinant Insulin-Like Growth Factor I Increases Insulin Sensitivity and Improves Glycemic Control in Type II Diabetes”. *Diabetes* - 1996; **45**: 91-100.
20. P. Sonksen, J. Sonksen Br. J. Anaesth. “Insulin: Understanding Its Action in Health and Disease”. *Oxford* - 2000; 85: 69-79.
21. E. Rinderknecht, R.E. Humbel. “The Amino Acid Sequence of Human Insulin Like Growth Factor I and Its Structural Homology with Proinsulin”. *The journal of Biological Chemistry* - 1978; **253**: 2769-2776.

22. Z. Laron. "Insulin a growth hormone". *Archives of Physiology and Biochemistry* - 2008; **114**: 11-16.
23. D.S. Straus. "Growth stimulatory action of insulin in vitro and in vivo". *Endocrine Reviews* - 1984; **5**: 356-369.
24. M. Gerald, A. D. Russell. "Antiseptic and Disinfectant: Activity, Action and Resistance". *Clinical Microbiology Reviews* - 1999; **12**: 147-179.
25. M. Albina, L. Bernd, T. William, M. David, V. Jillian, O. Gerald, B. Christopher, S. Gregory. "Bacterial Resistance Issues in Wound Care and Wound Dressing". *QuickMed Technologies* - 2009.
26. A. Shakeel , A. Mudasir, L.S. Babu, I. Saiqa . "A Review on Plant Extract Mediated Synthesis of Silver Nanoparticles for Antimicrobial Applications". *Journal of Advanced Research* - 2016; **7**: 17-28.
27. J.C. Pickup, Zheng-Liang Zhi, Faaizah Khan, Tania Saxl and D.J.S. Birch. "Nan medicine and its Potential in Diabetes Research and practice". *Diabetes/ Metabolism Research and Review* - 2008; **24**: 604-610.
28. Z.J. Jiang, Chun-Yan, Sun, L.W. Sun. "Catalytic Properties of Silver Nanoparticles Supported on Silica Spheres". *The Journal of Physical Chemistry B* - 2005; **109**: 1730-1735.
29. C. Philips, X. Hongliang and L. Suljo. "Visible-Light Enhanced Catalytic Oxidation Reactions on Plasmonic Silver Nanostructures". *Nature Chemistry* - 2011; **3**: 467-472.
30. K.A. Balkis, K. Rajasekar, T. Rajasekharan. "Silver Nanoparticles in Mesoporous Aerogel Exhibiting Selective Catalytic Oxidation of Benzene in CO_2 Free Air". *Catalyst Lett* - 2007; **119**: 289-295.
31. J.H. Liu, A.Q. Wang, Y.S. Chi, H.P. Lin and C.Y. Mou. "Synergetic Effect in an Au-Ag Alloy Nanocatalyst: CO Oxidation". *The Journal of Physical Chemistry B*- 2004, **109**: 40-43.
32. D. Peer, M. Jeffrey, S. Hong, C. Omid, Rimona, and R. Langer. "Nanocarriers as an Emerging Platform for Cancer Therapy". *Nature Nanotechnology* - 2007; **2**: 751-760.
33. H.J. Klasen. "A Historical Review of the Use of Silver in the Treatment of Burns". *Burns* 2000; **26**: 117-130.
34. C.P. Rajendra, R.V. Ram. "Comparative Volatile Oil Composition of Four Ocimum Species from Northern India". *Natural Research Product* - 2011; **25**: 569-575.
35. C. Diptiman, G. Arnab, G.D. Debabrata, R.A. Bipul, D. Amlan, C. Gopal."Apigenin shows synergistic anticancer activity with curcumin by binding at different sites of tubulin". *Biochime* - 2013; **9**: 1297-1309.
36. M. Poonam, M. Sanjay. "Antibacterial Activity of Ocimum Sanctum Extract against Gram Positive and Gram Negative Bacteria". *American Journal of Food Technology* - 2011, **6**: 336 - 341.
37. J. Liu. "Pharmacology of Oleanolic Acid and Ursolic Acid". *Journal of Ethnopharmacology* - 1995; **49**: 57-68.
38. N. Mahajan, S. Rawal, M. Verma, M. Poddar, S. Alok. "A Phytological Overview on Ocimum sanctum on Transient Cerebral Ischemia and Long-term Cerebral hypoperfusion". *Pharmacology, Biochemistry and Behaviour* - 2004; **79**: 155-164.
39. K.B. Birendra , K.P. Ashok. "Biosynthesis of silver Nanoparticles using *Ocimum sanctum* and Study of its Antimicrobial activity". *Journal of Nanoparticle Research* - 2011; **13**; 2981-2988J.
40. B.R. Acharya, B. Bhattacharyya, G. Chakrabarti. "The natural naphthoquinone plumbagin exhibits antiproliferative activity and disrupts the MT network through tubulin binding". A*merican Chemical Society*-2008; **47:** 7838-7845.

Figures

Absorbance (UV-Visible) Spectra

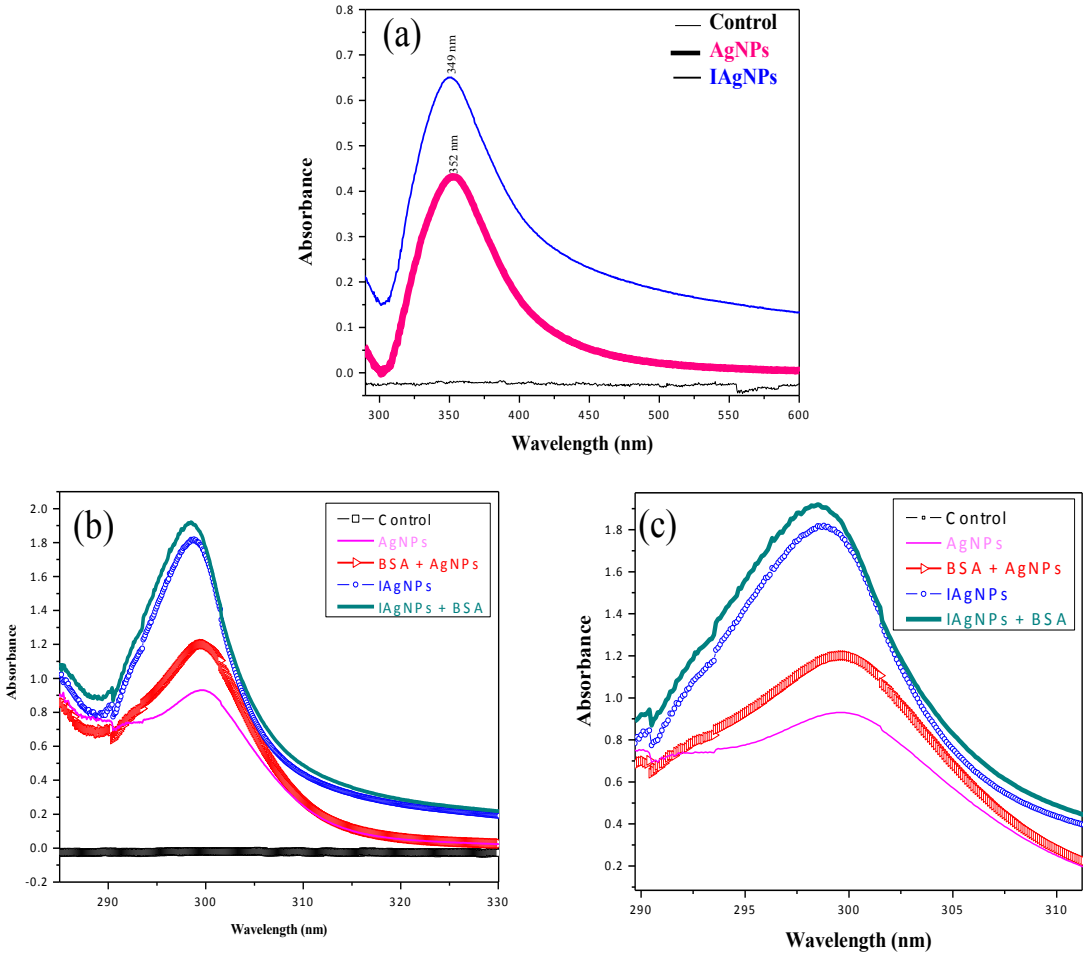

Fig 1 : UV- spectra (a) AgNPs and Insulin with AgNPs (IAgNPs) and (b) and (c) Control, AgNPs, AgNPs with BSA protein , Insulin with AgNPs and AgNPs with BSA and Insulin

Differential Light Scattering (DLS)

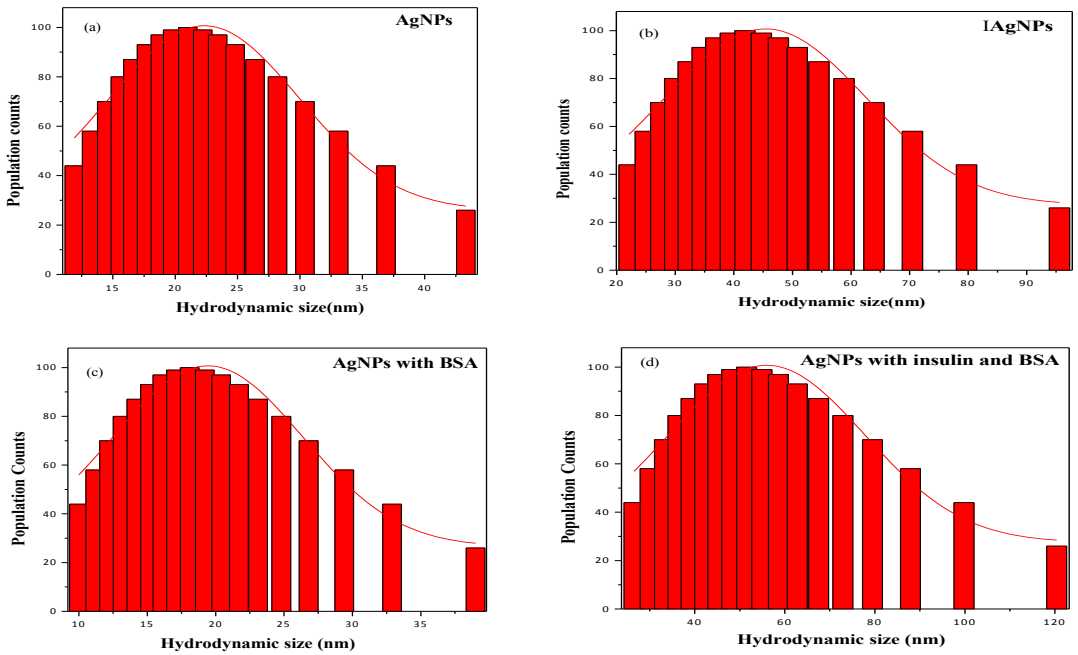

Fig 2: DLS shows hydrodynamic radius of (a) AgNPs (b) IAgNPs (c) AgNPs with BSA (d) AgNPs with BSA and Insulin

Far UV Circular dichroism (CD)

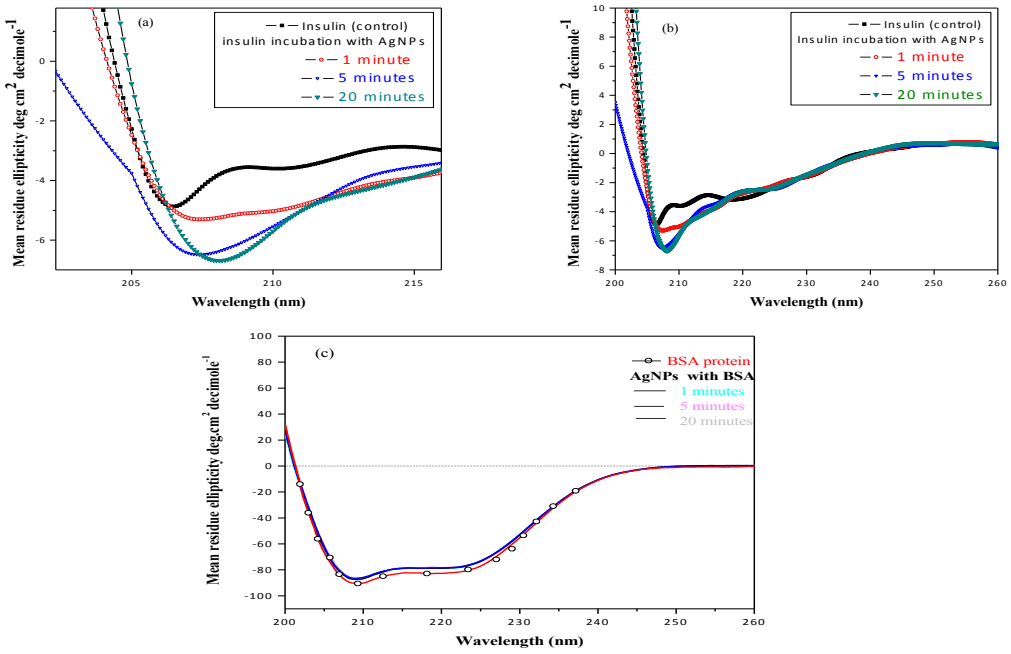

Fig 3: CD spectra of (a) & (b) Insulin with AgNPs (c) BSA with AgNPs (20 minute incubation) show secondary structure changes during binding

Fluorescence plot

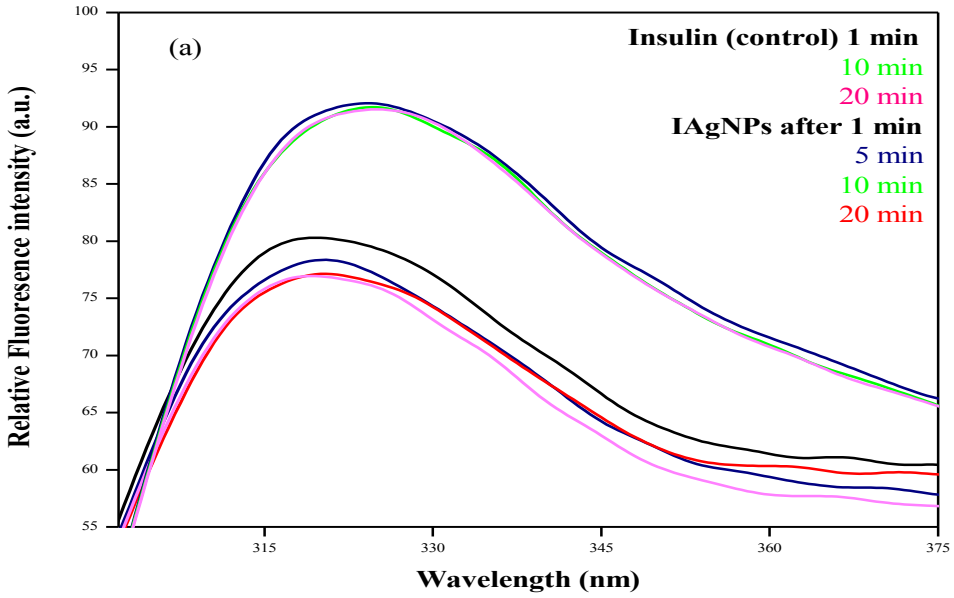

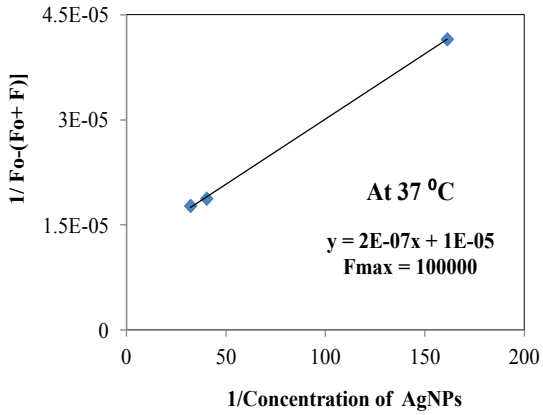

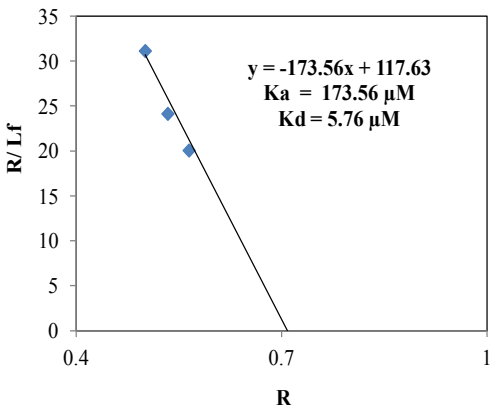

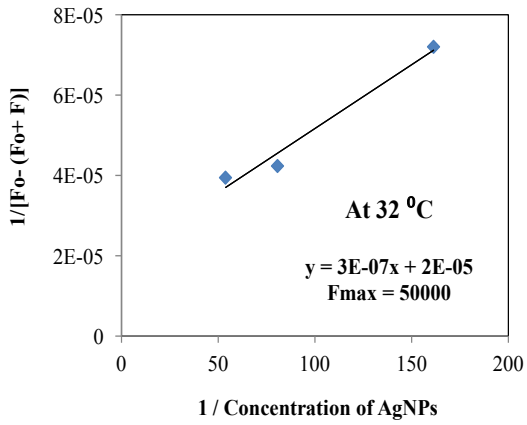

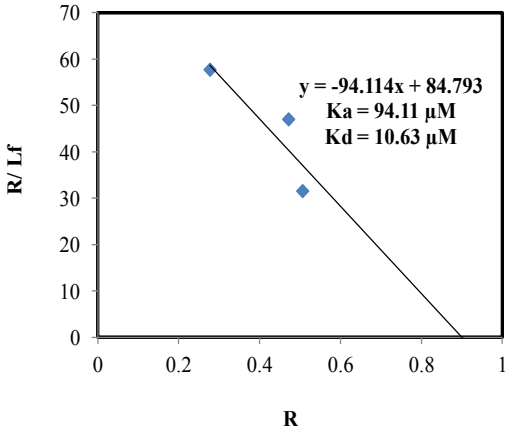

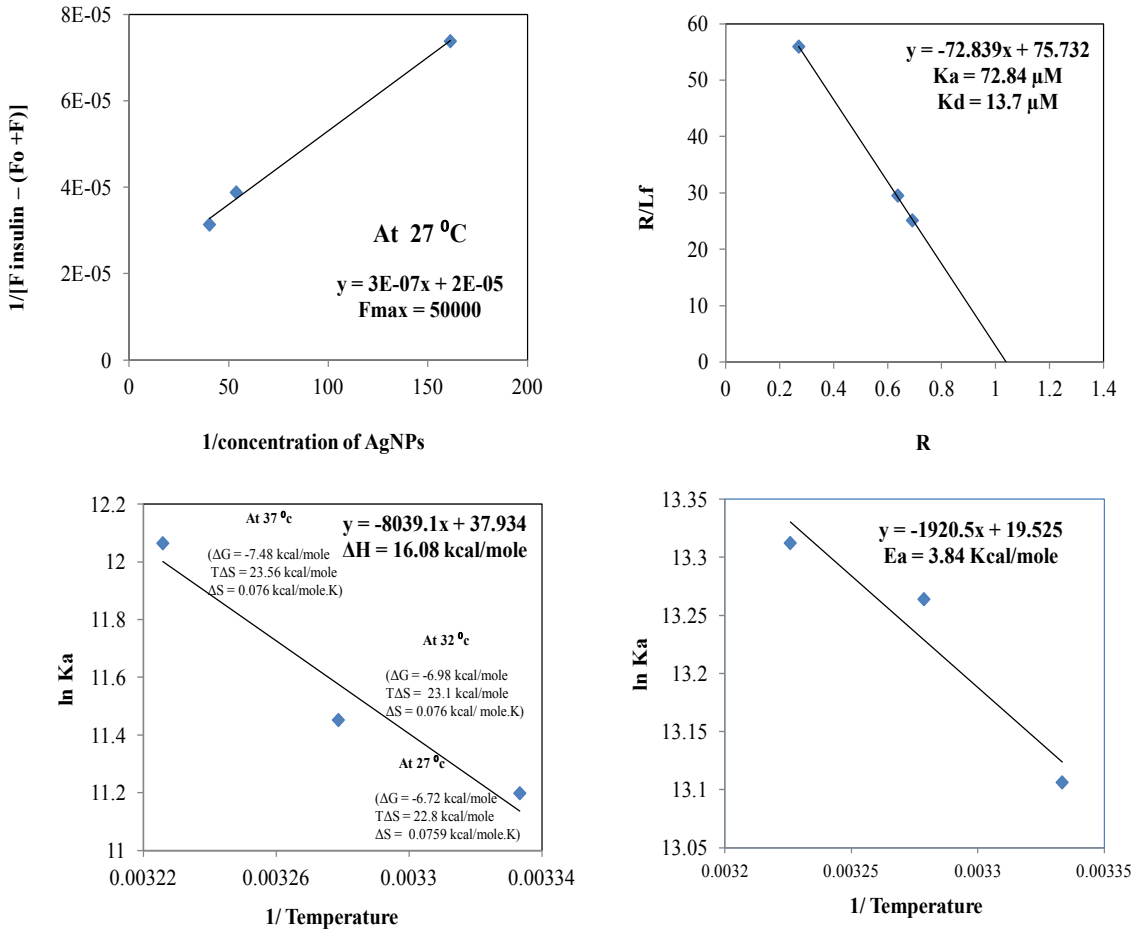

(b)

Fig 4: Fluorescence spectra (a) shows the time dependent quenching of tyrosine fluorescence of Insulin after incubation (b) At 37°C, 32°C, 27°C different kinetic parameters (K_a, K_d, Ea and stoichiometric binding) of binding of insulin with AgNPs

FTIR Spectra

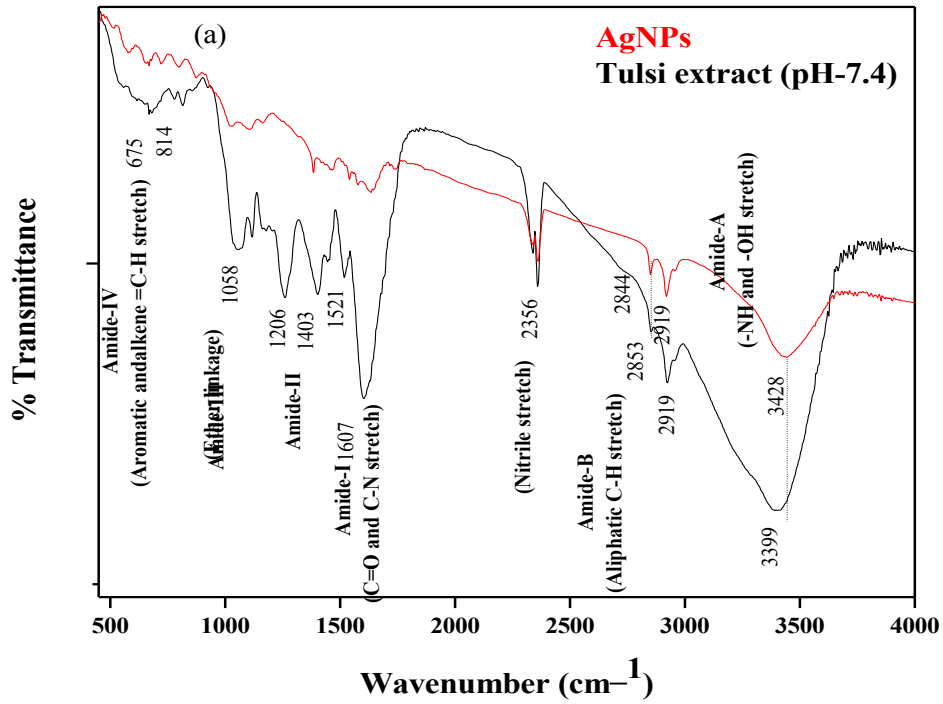

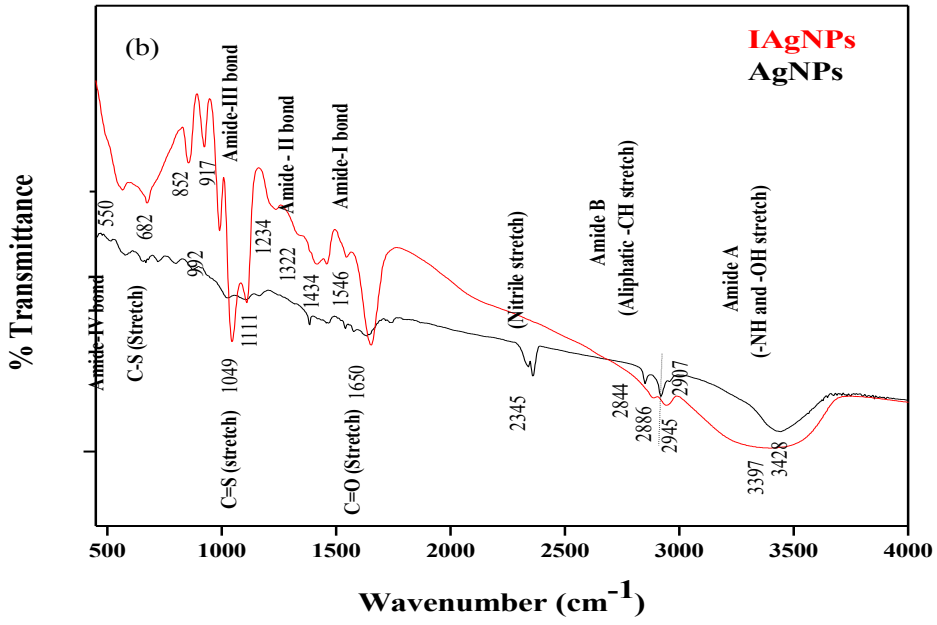

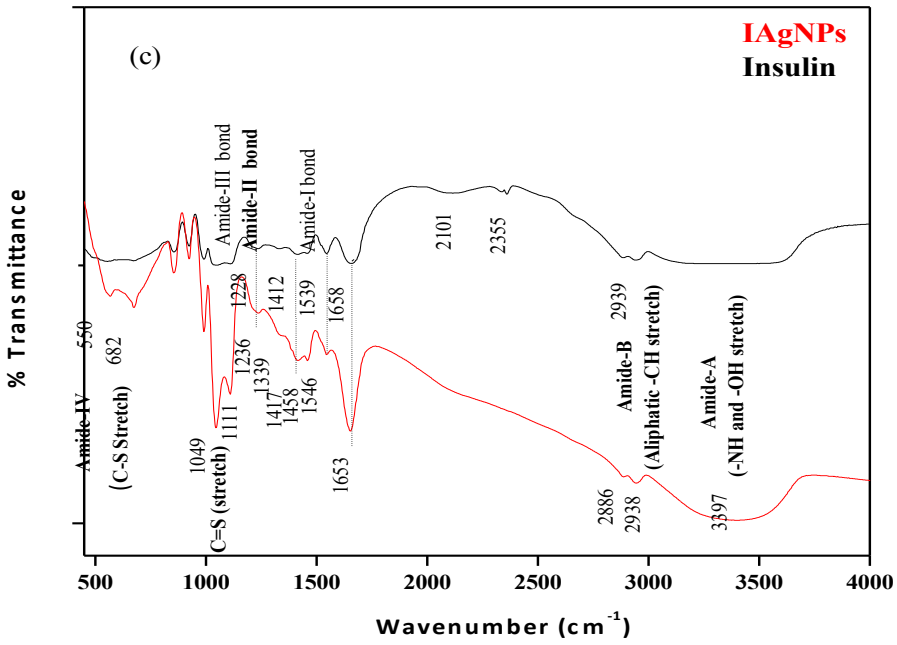

Fig 5 :FTIR spectra (Functional groups) (a) Comparison between AgNPs and TAE (b) AgNPs and IAgNPs (c) Insulin and IAgNPs

Raman spectra

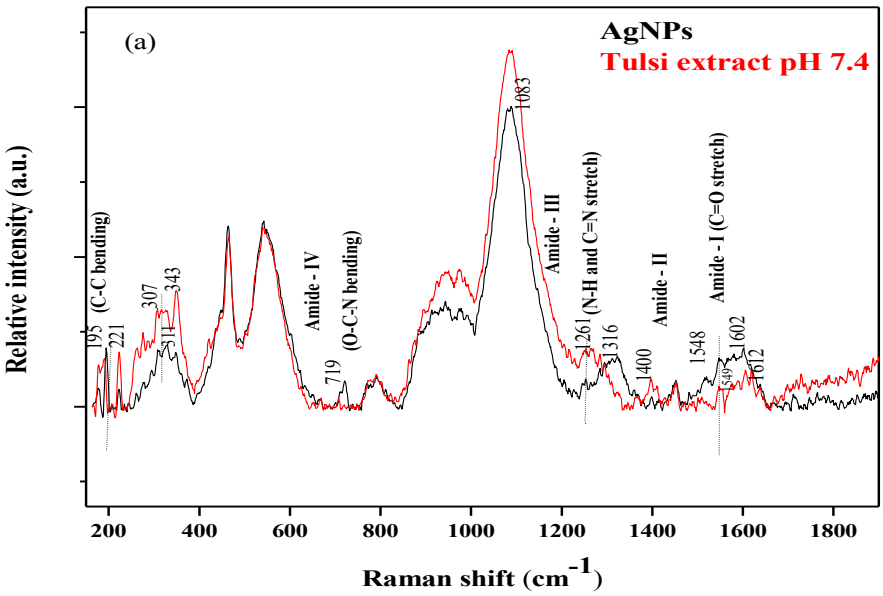

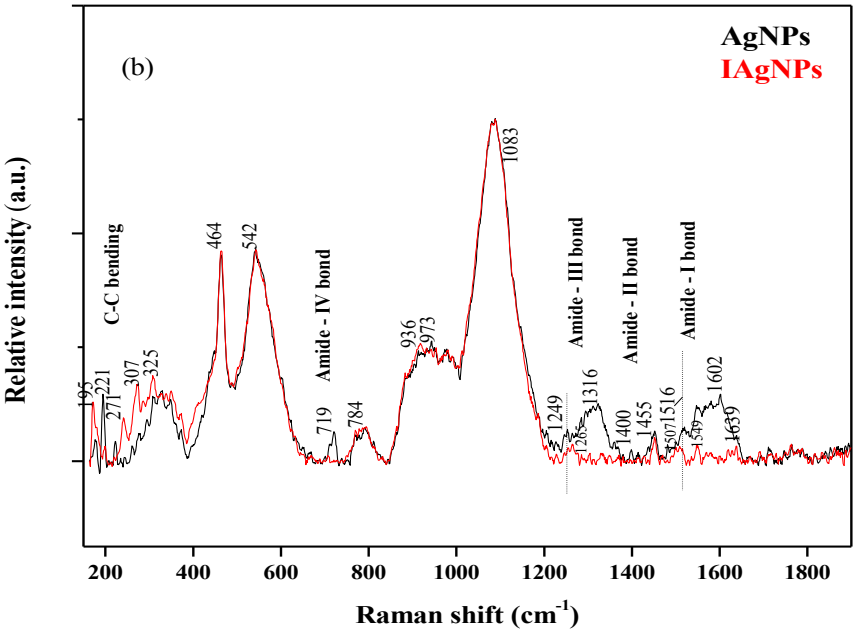
(b)
AgNPs
IAgNPs
Relative intensity (a.u.)
C-C bending
Amide - IV bond
Amide - III bond
Amide - II bond
Amide - I bond
195
221
271
307
325
464
542
719
784
936
973
1083
1249
1316
1400
1455
1516
1602
1639
200
400
600
800
1000
1200
1400
1600
1800
Raman shift (cm-1)

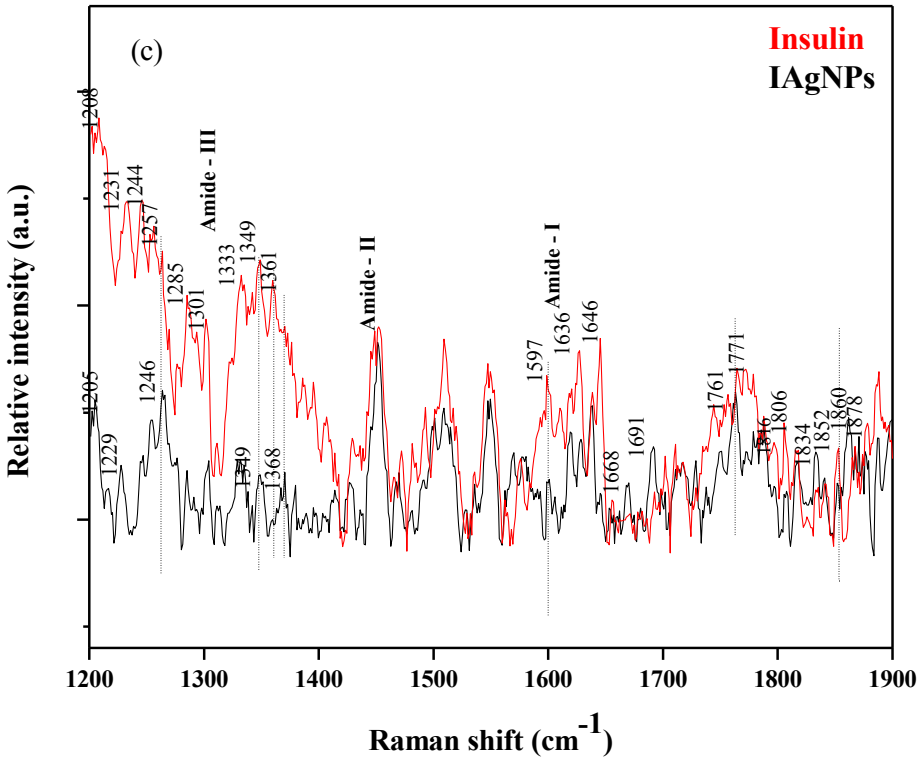
(c)
Insulin
IAgNPs
Relative intensity (a.u.)
Amide - III
Amide - II
Amide - I
1205
1208
1229
1231
1244
1246
1257
1285
1301
1333
1349
1349
1361
1368
1597
1636
1646
1668
1691
1761
1771
1806
1834
1852
1860
1878
1200
1300
1400
1500
1600
1700
1800
1900
Raman shift (cm-1)

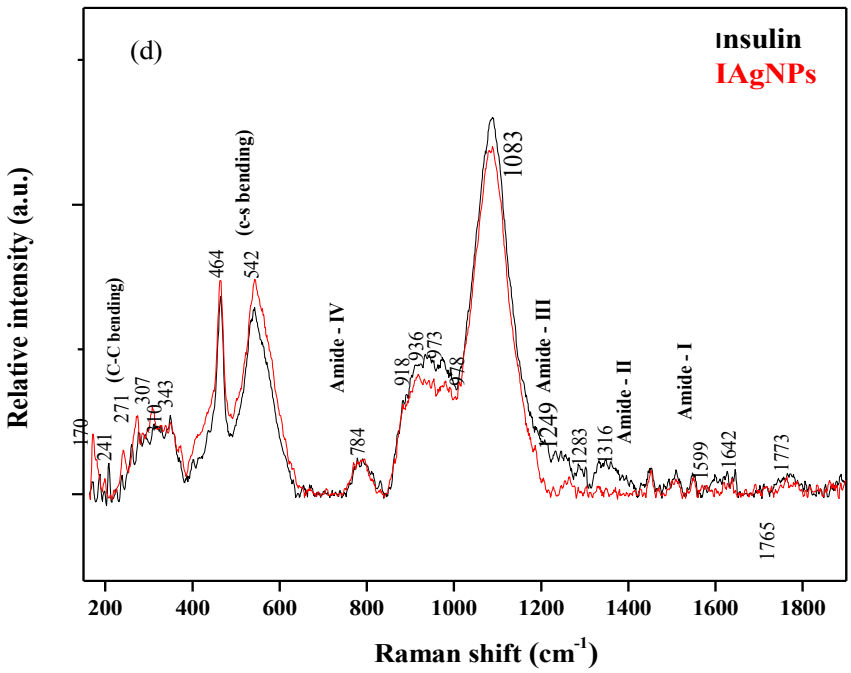

Fig 6: Raman spectra (Raman shift) (a) comparison of AgNPs and TAE (b) AgNPs and IAgNPs (c) and (d) Insulin and IAgNPs

SEM

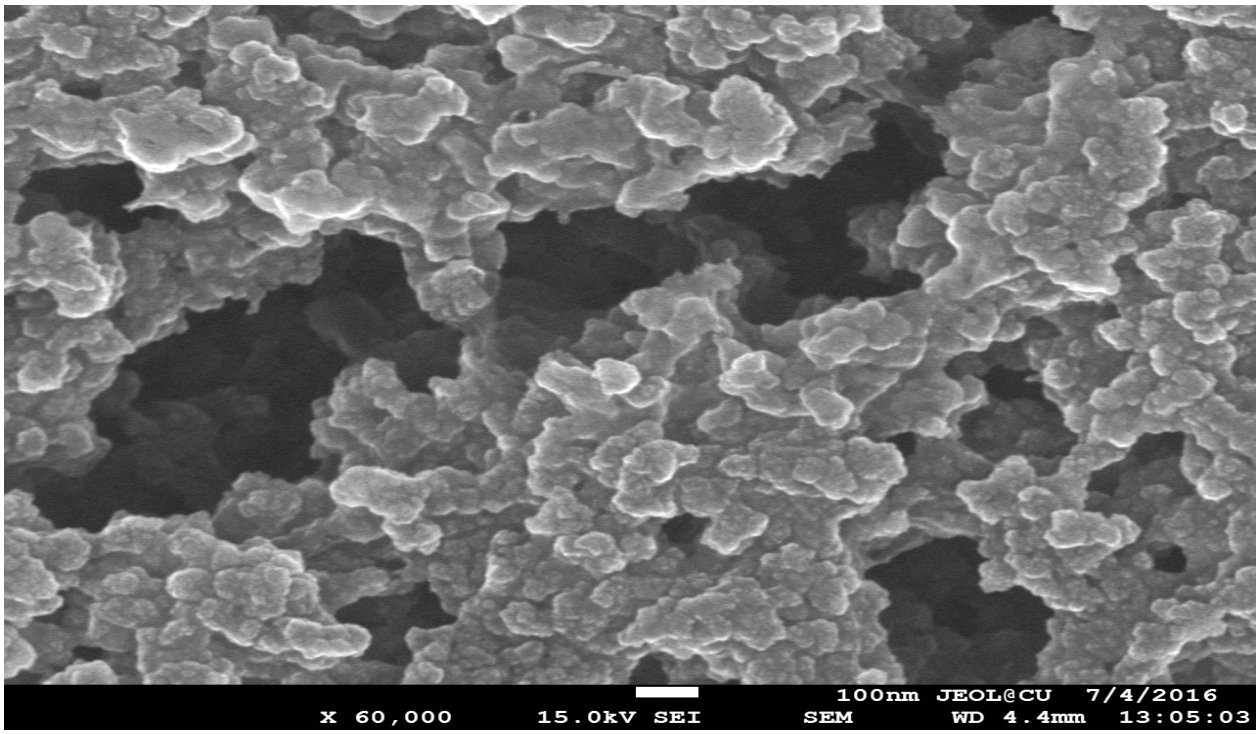

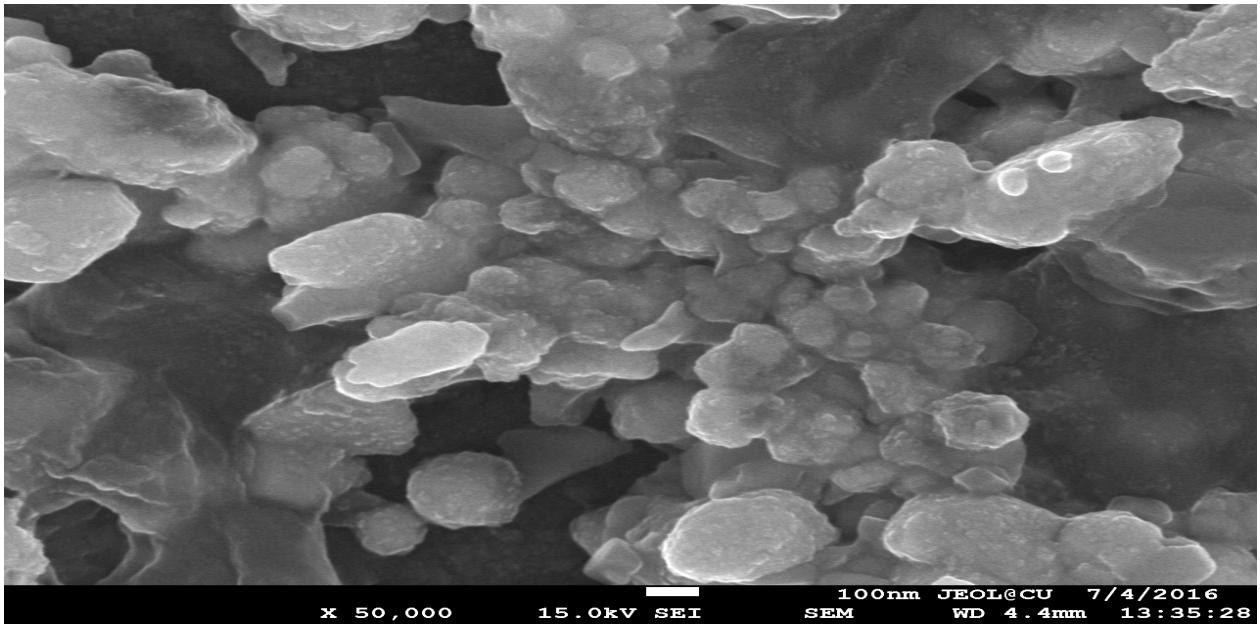

Fig 7: SEM images of (a) AgNPs (approximately 22 nm) and (b) IAgNPs (approximately 42 nm)

TEM micrograph

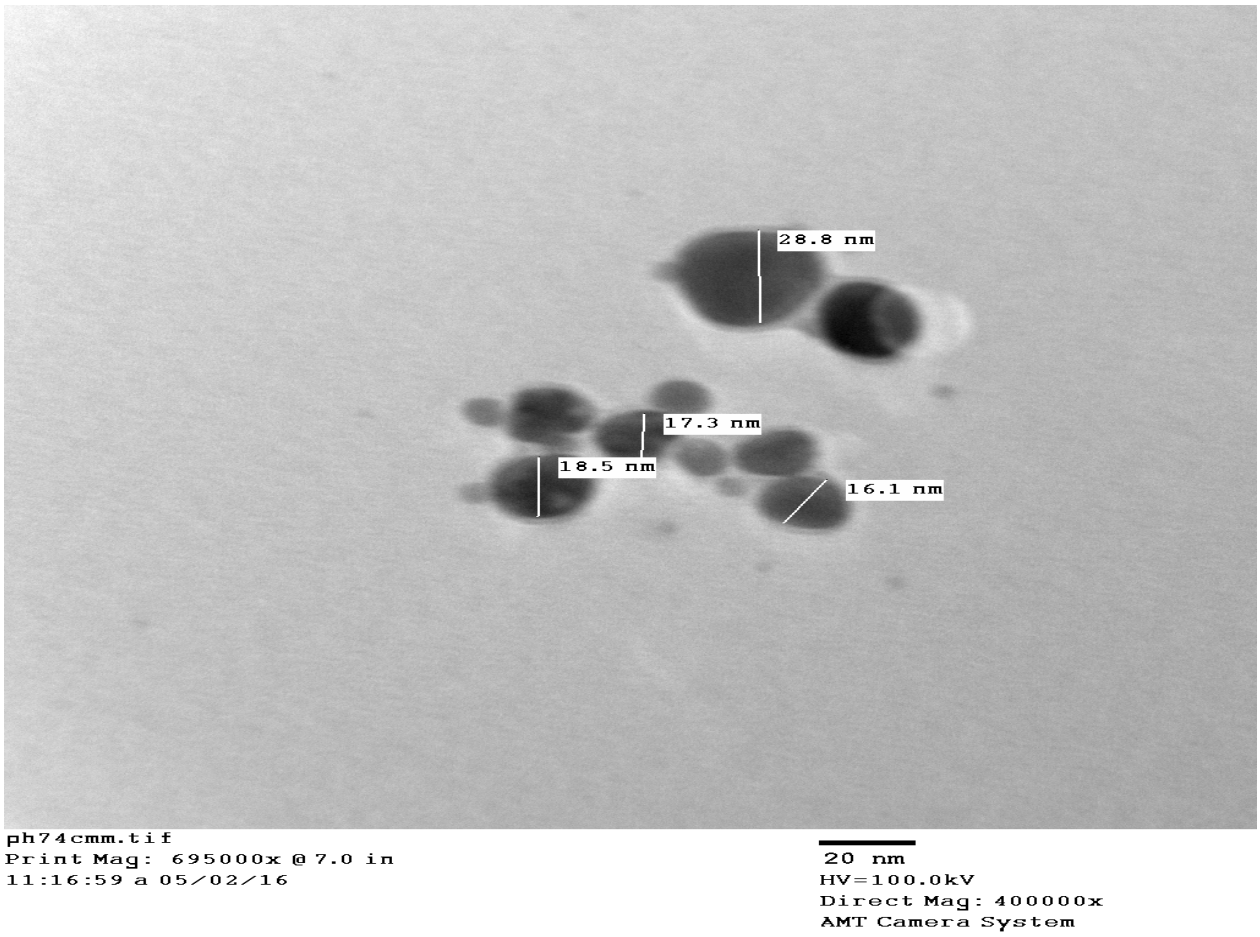

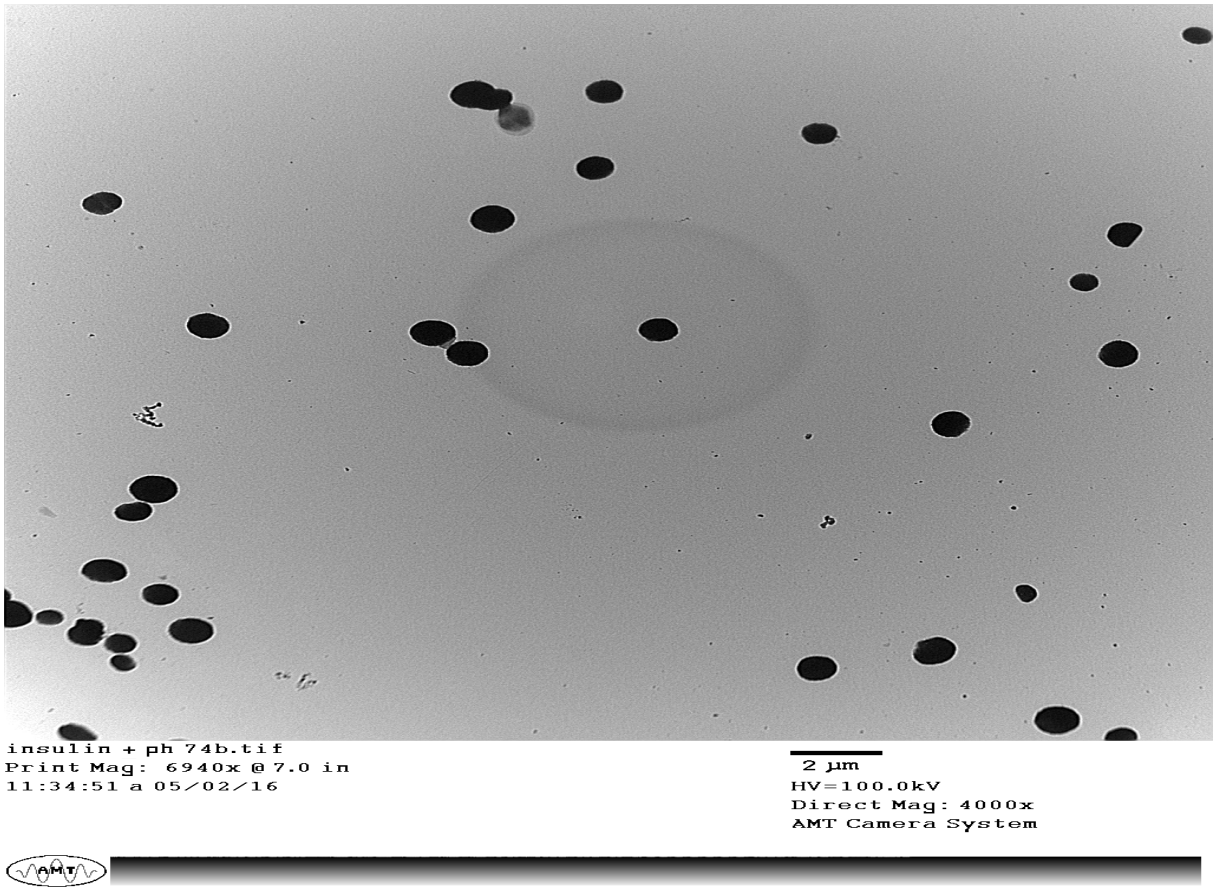

Fig 8: TEM micrographs (a) AgNPs and (b) IAgNPs

Lung epithelial cell line (A549)

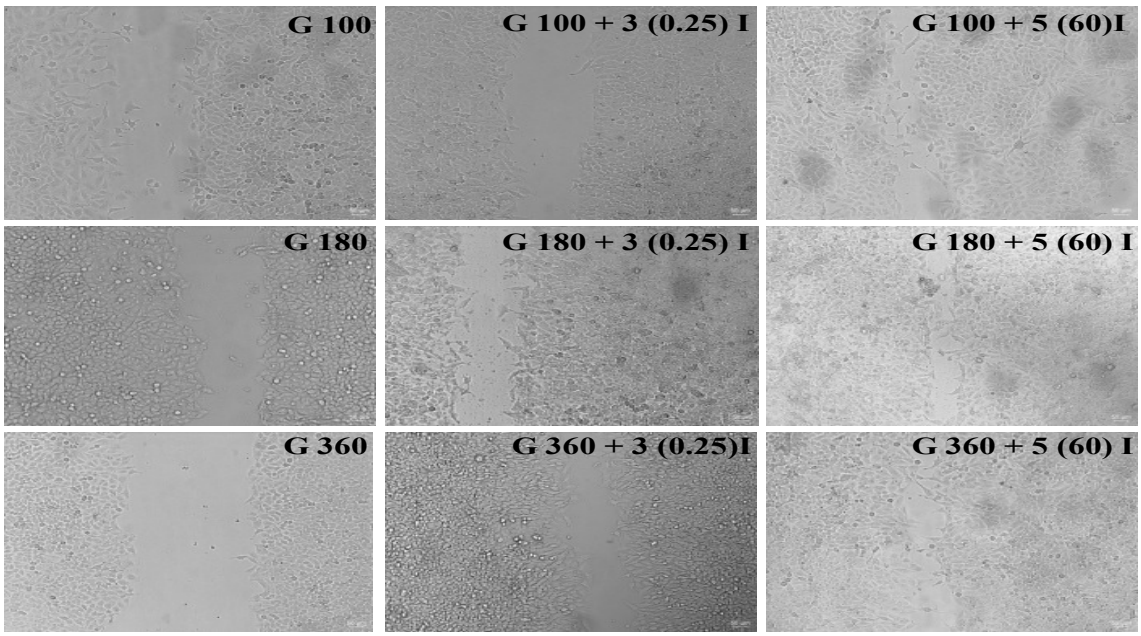

(a)

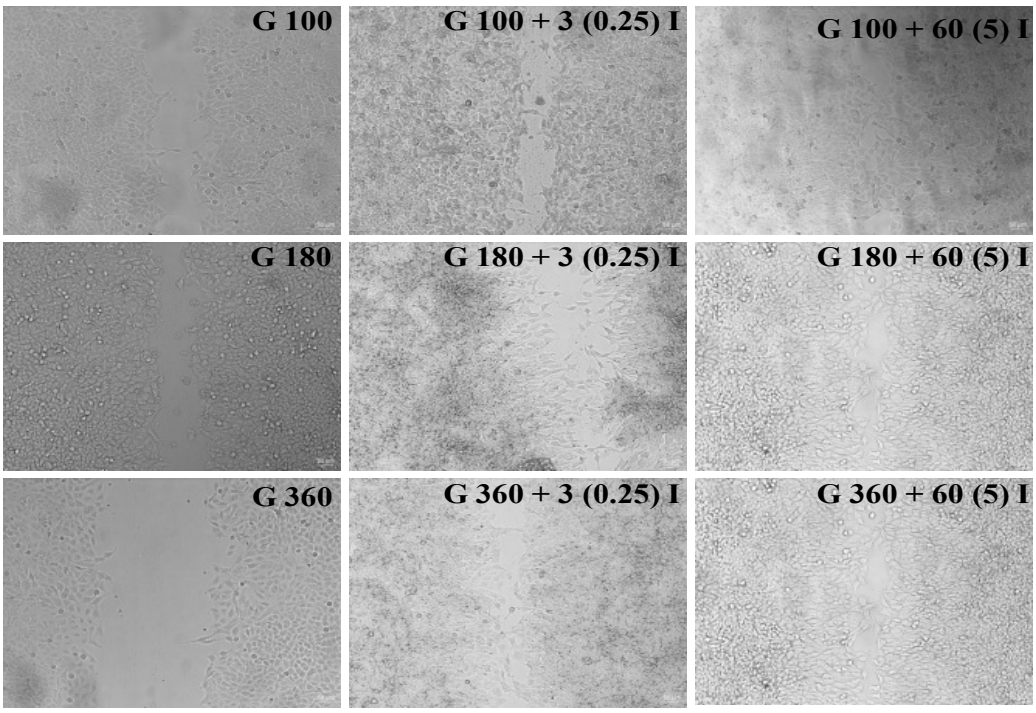

(b)

Fig 9: Lung epithelial cell (A549) migration (a) after 12 hours and (b) 24 hours